

The polymer phase of the TDAE-C₆₀ organic ferromagnet

Slaven Garaj¹, Takashi Kambe^{1,2}, László Forró¹, Andrzej Sienkiewicz³,
Motoyasu Fujiwara², Kokichi Oshima²

¹ *Institute of Physics of Complex Matter, École Polytechnique Fédérale de Lausanne, CH-1015 Lausanne, Switzerland*

² *Graduate school of natural science and technology,*

Okayama University, 3-1-1 Tsushima, Okayama 700-8530, Japan and

³ *Institute of Physics, Polish Academy of Sciences, 02-668 Warsaw, Poland*

(Dated: November 19, 2018)

The high-pressure Electron Spin Resonance (ESR) measurements were performed on TDAE-C₆₀ single crystals and stability of the polymeric phase was established in the $P - T$ parameter space. At 7 kbar the system undergoes a ferromagnetic to paramagnetic phase transition due to the pressure-induced polymerization. The polymeric phase remains stable after the pressure release. The depolymerization of the pressure-induced phase was observed at the temperature of 520 K. Below room temperature, the polymeric phase behaves as a simple Curie-type insulator with one unpaired electron spin per chemical formula. The TDAE⁺ donor-related unpaired electron spins, formerly ESR-silent, become active above the temperature of 320 K and the Curie-Weiss behavior is re-established.

PACS numbers: 71.20.Tx, 75.50.Dd, 76.50.+g, 73.61.Ph

I. INTRODUCTION

The organic charge-transfer compound TDAE-C₆₀ (where TDAE is tetrakis-dimethylamino-ethylene) is a ferromagnet with the Curie transition temperature of $T_C = 16$ K (Ref. [1]). This is the highest temperature onset of ferromagnetic behavior for a purely organic material. It is customarily accepted that the system is an isotropic Heisenberg ferromagnet with an extremely small anisotropy field[2][3].

The TDAE molecule, a strong electron donor, transfers one electron to the lowest unoccupied molecular orbital (LUMO) of C₆₀ in a similar way to that found in alkali metal C₆₀ compounds. It has been established that the single-charged C₆₀ alkali salts, A₁C₆₀ (A= K, Rb, Cs), reveal metallic properties in a wide temperature range[4]. Although, analogously to the alkali metal C₆₀ compounds, the valence band in TDEA-C₆₀ originates from the triply degenerated t_{1g} orbital of the C₆₀ molecule, the TDAE-C₆₀ system was found to be non-metallic[5][6]. The non-metallic behavior of TDAE-C₆₀ was explained assuming the Jahn-Teller effect and Mott-Hubbard localization[7][8].

Magnetic susceptibility measurements[9][10][11] as well as Electron Spin Resonance (ESR) results[11][12] showed that the TDAE-C₆₀ system has only one $S = 1/2$ magnetic moment per chemical formula unit. From the g -factor analysis it was concluded that the spins are mainly localized on C₆₀⁻ (Ref. [11]). The TDAE⁺ donors should also carry non-paired electrons. However, these centers remain ESR silent, which is probably due to the mechanism of the spin-singlet pairing resulting from the dimerization shift of the neighboring TDAE⁺ molecules[13].

Two magnetic variants of TDAE-C₆₀ were discovered. As grown crystals (α' -phase) reveal the antiferromagnetic (AFM) behavior, whereas annealed crystals (α -phase) show the transition to the ferromagnetic (FM) state[14].

Surprisingly, in X-ray diffraction (XRD), these two structures look almost indistinguishable around the room temperature when the C₆₀ balls rotate freely. However, the difference is observed when freezing of the rotation of the C₆₀ balls occurs at low temperatures[12][15]. In the FM phase, a new Bragg reflection develops, suggesting lowering of symmetry and ordering of the C₆₀ balls[12]. This reflection is not observed in the AFM phase, which suggests the existence of a disordered (glassy) state of the C₆₀ orientations.

Nuclear Magnetic Resonance (NMR) data imply that in the FM phase the electron spin of C₆₀⁻ are partially delocalized on the TDAE molecule, thus raising a possibility for the super-exchange interaction[16]. In a simple model, one would expect that the super-exchange mechanism would promote the AFM behavior. Nevertheless, the observed ferromagnetic properties are explained in terms of the Hubbard model with the antiferro-orbital order of the Jahn-Teller distorted (JTD) C₆₀ balls[8]. Indeed, NMR observations of the JT distortion and the asymmetric charge distribution on the C₆₀ balls have recently been reported[17]. However, the NMR results of Arcon et al.[16] suggest that the α -phase contains the C₆₀⁻ molecules with both ferromagnetic and antiferromagnetic configurations. In that case, the spontaneous magnetization should appear when the concentration of the FM configuration is high enough for the appearance of an infinite ferromagnetic cluster through percolation mechanism[15][18].

Recently, Mizoguchi and co-workers[19] reported polymerization of TDAE-C₆₀ under pressure of ~ 10 kbar. The polymerized phase (β -phase) remains stable even after releasing the pressure. The polymerization process occurs along the c -axis and it has been suggested that the linear polymers can be formed due to a [2+2] cycloaddition process.

In this article, we report the $P - T$ diagram of the sta-

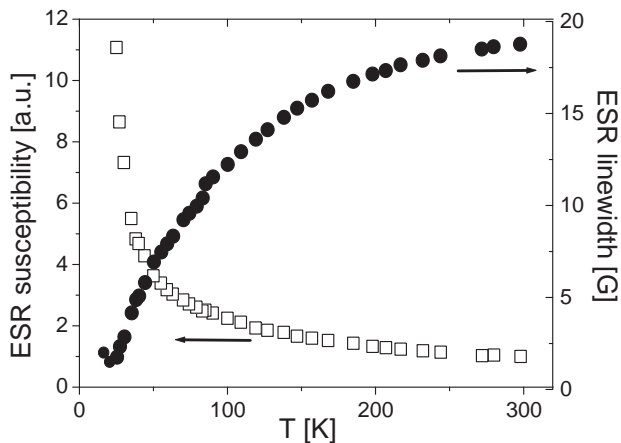


FIG. 1: Spin susceptibility (left scale, open squares) and the ESR linewidth (right scale, filled circles) of the ferromagnetic TDAC- C_{60} single crystal as a function of temperature. In the ferromagnetic region below $T_C = 16$ K, the linewidth cannot be easily defined because the line shapes are strongly distorted due to mosaicity of the crystal

bility of the polymeric TDAC- C_{60} structure. The effects of the high-hydrostatic pressure on the physical properties of both monomeric and polymeric phases were investigated. We studied the physical properties of the β -phase at low and high temperatures and the effect of the temperature-induced depolymerization. The properties of the TDAC- C_{60} polymer are compared with those of other bonded fullerene structures.

II. EXPERIMENT

Single crystals of the TDAC- C_{60} were prepared by the diffusion method as reported in Ref. [12]. The single crystals dimensions were, typically, of $0.3 \times 0.3 \times 0.3$ mm³. The presence of the FM phase was checked by the magnetization measurements.

Ambient pressure Electron Spin Resonance (ESR) measurements were performed in the temperature range of 5 – 600 K using a Bruker ESP300E X-band spectrometer. In the temperature range of 5 – 300 K the ESR spectra were acquired using a standard Bruker TE₁₀₂ cavity that was equipped with an Oxford Instrument, Model ESR900, gas-flow cooling system. In the upper temperature range (300 – 600 K) we used a Bruker ER4114HT high-temperature cavity system. The magnetic field and the microwave frequency were calibrated using a commercially available NMR gauss-meter and a frequency counter, respectively. The ESR line intensities were calibrated using a secondary standard sample, a small speck of DPPH (2,2-diphenyl-1-picrylhydrazyl from Sigma).

The high-pressure ESR measurements were performed using a high-pressure system that was recently developed at the EPFL. The high-pressure ESR probe was designed as an interface to our Bruker ESP300E X-band spec-

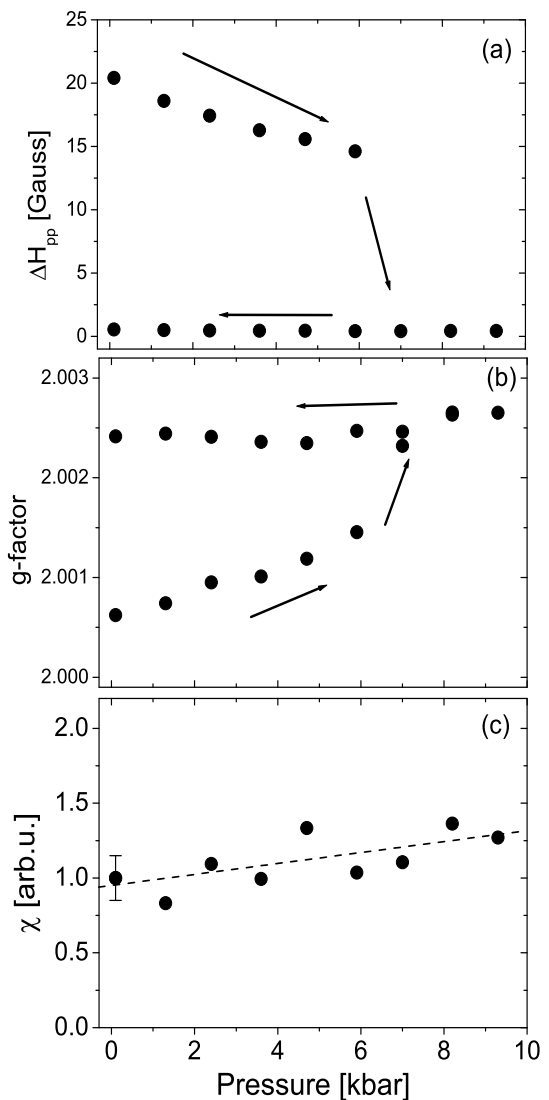


FIG. 2: Pressure dependence of the ESR parameters for single crystal TDAC- C_{60} at room temperature: (a) linewidth; (b) g -factor; (c) relative spin susceptibility. Phase transition to the polymerized phase is visible at $P_C = 7$ kbar.

trometer. The probe consists of two sub-assemblies: 1) the microwave resonant structure containing the double-stacked Dielectric Resonator (DR) and 2) the miniature sapphire-anvil pressure cell (SAC). The SAC is ruby-calibrated; thus the hydrostatic pressure can be monitored in situ by detecting the pressure-induced shift of the red fluorescence of Cr^{3+} ions in a small crystal of ruby. The commercially available "Daphne" oil was used as a pressure-transmitting medium. In this work, the maximum applied pressure was of 9 kbar. For performing low temperature measurements, the high-pressure probe was inserted into the CF-1200 Oxford Instrument gas-flow cryostat operating in the 5 – 290 K temperature range. The details of the DR-based high-pressure ESR probe will be published shortly elsewhere [20]. The ESR line

intensities and the g -factor were calibrated using an additional reference sample, a polycrystalline MnO/MgO, which was positioned in the active zone of the microwave resonant structure (close to the gasket of the SAC).

III. RESULTS

A. Pressure-induced polymerization

Figure 1 shows the temperature evolution of the ESR-probed spin susceptibility and the ESR linewidth of the ferromagnetic phase of TDAE-C₆₀ measured at ambient pressure. In the ferromagnetic region, below $T_C = 16$ K, the linewidth cannot be determined precisely due to the strong distortion of the ESR line shape. The line shape distortion is probably due to the non-homogeneity of the local internal fields in different ferromagnetic domains of the crystal.

The pressure dependence of the ESR linewidth (peak-to-peak, ΔH_{pp}) of TDAE-C₆₀ at ambient temperature is shown in Fig. 2a, whereas Fig. 2b shows the pressure dependence of the g -factor. The initial (ambient pressure) linewidth of $\Delta H_{pp} \approx 20$ G slowly decreases with increasing pressure to 15 G at $P = 6$ kbar. Then, at $P_C = 7$ kbar, a transition to the polymeric phase is clearly seen as a sudden drop in the ESR linewidth (Fig. 2a). This is also accompanied by an abrupt change (increase) in the g -factor (Fig. 2b). The phase transition is irreversible and the polymeric phase remains stable after releasing the pressure. These results are in a partial agreement with the ESR measurements performed at lower microwave frequencies by Mizoguchi et al.[19]. The major difference is, however, that the critical pressure of suppression of the ferromagnetic transition in our measurements is rather lower and coincides with the pressure of the complete polymerization.

In the monomeric TDAE-C₆₀ the ESR linewidth is defined by dipolar interaction with additional narrowing introduced by the exchange interaction. Accordingly, as can be seen in Fig. 2a, the monomer's linewidth slowly narrows with pressure approaching 7 kbar. This is due to the larger overlap of the electronic wave functions, which leads to an enhanced exchange interaction. At ambient pressure, the g -factor value for the monomeric phase of TDAE-C₆₀ is 2.0006 and is distinctively closer to the g -factor of the fullerene anion C₆₀⁻ ($g_{C_{60}^-} = 1.9998$) than to the g -factor value that is characteristic for the TDAE⁺ cation ($g_{TDAE^+} = 2.0036$). This is due to the fact that the ESR signal originates from the electrons that are mainly localized on the C₆₀ balls. The spins on the TDAE⁺ radicals are ESR-silent, which is probably due to a slight dimerization of TDAE molecules, thus yielding a spin-singlet configuration. With increasing pressure, the g -factor linearly increases towards the value of the TDAE⁺ cation. This implies that the unpaired spin density is spreading towards the TDAE molecule with increasing pressure.

At $P_C = 7$ kbar, a sudden narrowing of the ESR line is visible due to polymerization. The linewidth drops by two orders of magnitude, reaching $\Delta H_{pp}(\text{polymer}) = 0.5$ G. The narrow linewidth and the Currie type temperature dependence of the spin susceptibility at this pressure suggest that the polymeric phase is non-metallic. Upon polymerization the g -factor value rises reaching 2.0024 and becomes almost pressure independent.

Mizoguchi et al.[19] suggested that the polymerization process decouples the previously ESR-silent spins related to the TDAE⁺, which should lead to an effective doubling of the total number of spins. The observed pressure dependence of ESR susceptibility at room temperature (Fig. 2c) does not support this suggestion. At this stage, a small increase (of $\sim 20\%$) of the ESR susceptibility upon polymerization can be explained by the differences in the Weiss temperatures between the two phases.

B. Coexistence of phases

Figure 3 shows the temperature dependence of the ESR linewidth and the g -factor for three different pressures. The temperature dependence of the linewidth and the g -factor at applied pressure of $P = 2.6$ kbar is shown in Fig. 3a and Fig. 3b, respectively. As can be seen in Fig. 3a, below the characteristic temperature, $T_P = 100$ K, in addition to the ESR line of TDAE-C₆₀ monomer (full circles), a new line appears (open circles). This new ESR line can be assigned to the polymeric phase while taking into account the g -factor and ESR linewidth evolution with pressure. The intensity of the polymeric line does not exceed 15% of the intensity of the monomeric line. The temperature dependence of the g -factor and ESR linewidth at $P = 4.7$ kbar is shown in Fig. 3c and Fig. 3d, respectively. At this pressure, a partial polymerization starts at higher temperatures, around $T_P \approx 180$ K. The intensity of the polymeric line is now much more pronounced. For both applied pressures, the monomeric phase undergoes the ferromagnetic phase transition, whereas the polymeric phase does not. At pressure of $P = 7.0$ kbar, the sample is fully polymerized already at room temperature (Fig. 3e and Fig.3f). No ferromagnetic phase transition is visible down to 5 K. At this applied pressure, the ESR susceptibility follows a simple Curie law, without a detectable Weiss constant. The ESR linewidth is very narrow (0.5 G) and is almost independent of temperature, whereas the g -factor slightly changes with temperature.

The stability of the polymer phase in the $P - T$ parameter space is depicted in Fig. 4. The polymerization temperature (T_P) has a linear dependence with applied pressure, where the proportionality constant. The ratio of the polymeric and monomeric ESR line intensities depends not only on pressure, but also on temperature. To deduce the exact structural dynamics of the polymer formation an additional structural study is needed.

The pressure dependence of the ferromagnetic tran-

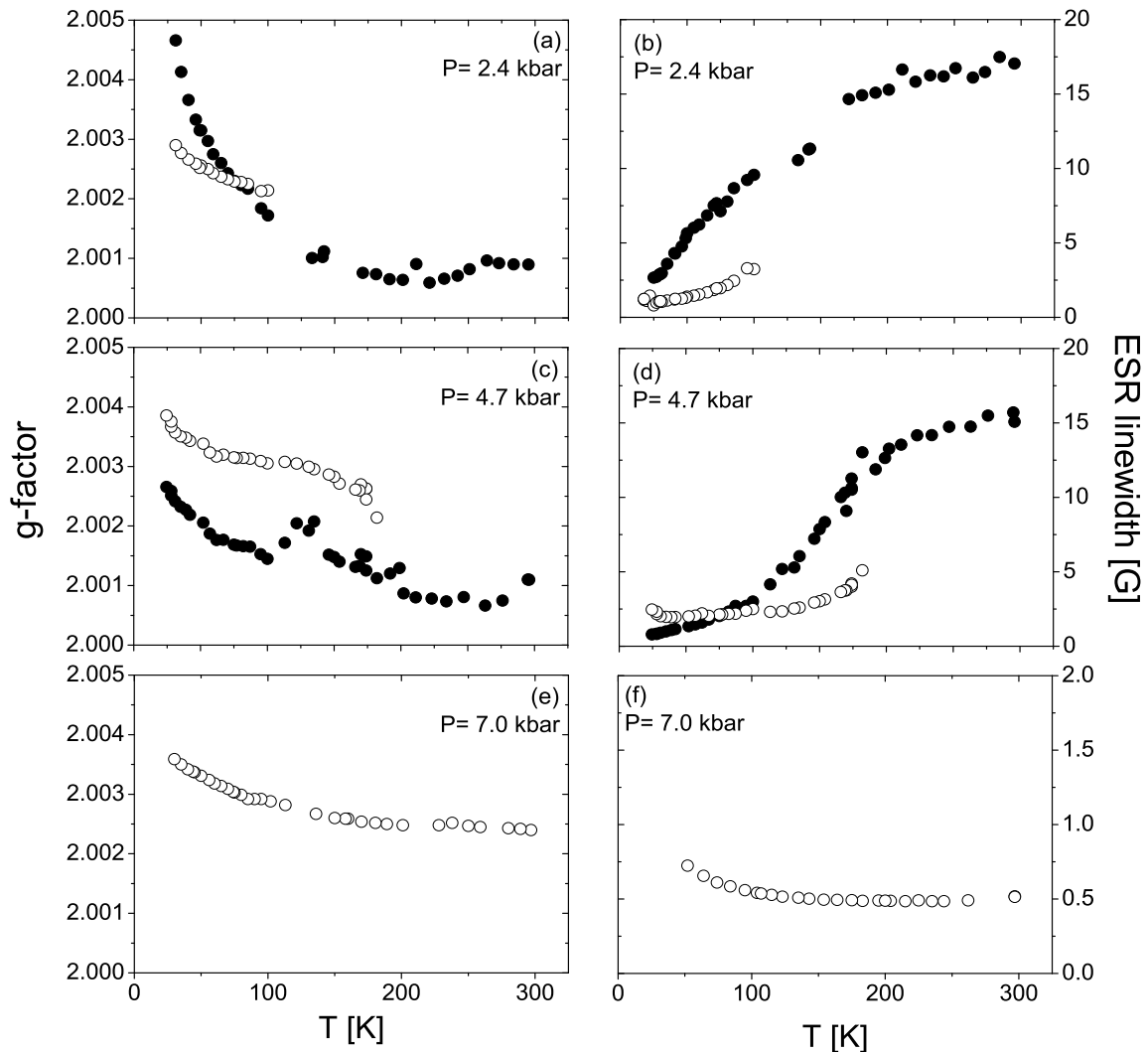


FIG. 3: Temperature dependence of the ESR linewidth and the g -factor for the pressures of 2.6 kbar (a, b), 4.7 kbar (c, d,) and 7 kbar (e, f). Below the polymerization temperature, in addition to monomeric line (filled circles), a new line appears (open circles) which was assigned to polymer. At 7 kbar the system is fully polymerized at the room temperature.

sition temperature (T_C) of the monomeric phase is depicted in Fig. 5. To determine T_C , we cannot compare the resonance field shift with the conventional Bloch's law, because the resonance field has pronounced temperature dependence even above T_C (see Fig. 3). This shift is due to the demagnetization effects, which depend on the sample shape[21]. Concomitantly, we define T_C as the onset temperature of the broadening of a linewidth distribution of the monomer-related ESR features (see: inset to Fig. 5). This linewidth distribution broadening is due to the growth of an internal field below T_C and the mosaicity of the crystal. The observed pressure dependence of T_C is similar to the parabolic dependence reported in Ref. [19]. However, in contrast to their ESR data acquired at low microwave frequencies and fields, the ferromagnetic transition observed in this work vanishes simultaneously with polymerization. This result

can be expected and explained in the framework of the theory by Kawamoto and coworkers[8], because the onset of polymerization prevents the antiferro ordering of the orbital of the JTD fullerene molecules.

C. Polymer phase at ambient pressure

The polymeric phase remains stable even after the pressure is released. For the polymeric phase, the temperature dependences of the ESR parameters are shown in Fig. 6. As can be seen from comparison of the results presented in Fig.6 and in Fig. 3a and Fig. 3b, the low-temperature properties of the polymeric phase at ambient pressure are very similar to those observed at $P = 7$ kbar. The temperature dependence of the inverse ESR susceptibility, χ^{-1} , of the polymeric phase is shown in

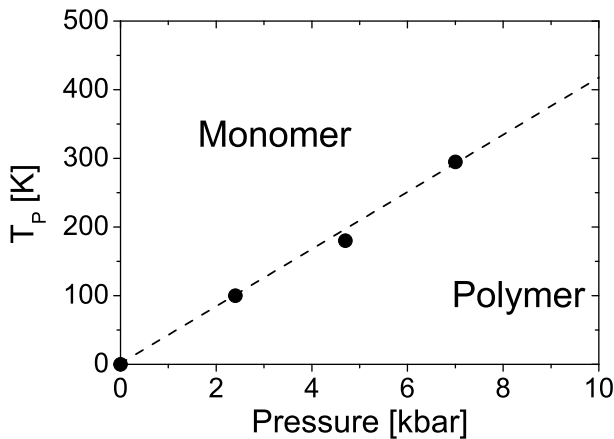


FIG. 4: Polymerization temperature (T_P) as a function of applied pressure. The polymerization temperature has a linear dependence on the applied pressure, with the constant of proportionality of $\frac{dT_P}{dP} = 41 \pm 2$ K/kbar

Fig. 6a. Since we are dealing with localized spins, this type of plot (χ^{-1} vs. T) is the most informative, directly yielding information on the Curie constant and the Weiss temperature of the system. The spin susceptibility below the room temperature reveals one spin $S = 1/2$ per chemical formula unit ($N = 1$) and a simple Curie behavior.

As seen in Fig. 6a, the inverse susceptibility departs from the simple Curie behavior at 260 K. This transition region is relatively broad and extends up to ca. 320 K. Above 320 K, the ESR susceptibility reveals the doubling of the number of spins per chemical formula. This phenomenon can be understood in terms of re-appearance of the previously hidden spins of the TDAE⁺ radicals. The Weiss temperature does not vanish anymore, having the value of $\Theta = 230 \pm 20$ K. This change of behavior at high temperatures is also seen in the temperature dependence of the linewidth (Fig. 6b). At lower temperatures the ΔH_{pp} is almost constant, with a slight tendency to decrease with increasing temperature, whereas above the room temperature it changes its slope and starts to increase more rapidly. The temperature dependence of the g -factor (Fig. 6c) reveals a similar, distinctive change of behavior above the room temperature.

The polymeric phase remains stable up to the depolymerization temperature, $T_{DP} = 520$ K. Above this temperature, both the ΔH_{pp} and the g -factor recover their characteristic values for the ferromagnetic phase (Fig. 7). The depolymerization process is an irreversible transition. At the depolymerization temperature, both polymeric and ferromagnetic ESR features are present, thus pointing to the coexistence of the two phases. It also suggests that this phase transition does not seem to be an abrupt one. As in the case of ferromagnetism, the polymerization process might be influenced by percolation mechanism, as the samples of apparently lesser quality exhibit a bit lower depolymerization temperature.

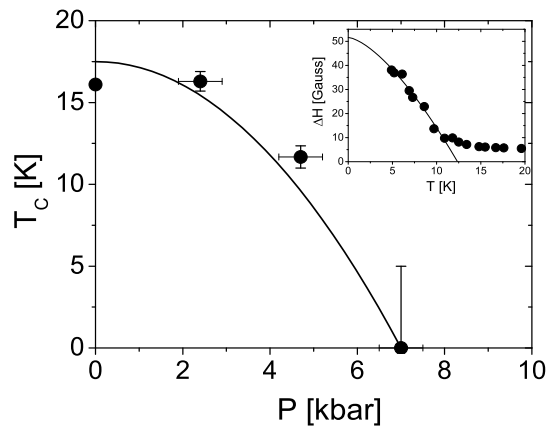


FIG. 5: Pressure dependence of the ferromagnetic transition temperature, T_C , for single crystal TDAE-C₆₀. T_C at each pressure is determined by the onset temperature of the broadening of the linewidth distribution of the monomeric signal. The lines are guides for the eye. Inset: line distribution broadening for the pressure of 4.6 kbar.

At low temperatures, the depolymerized crystals reveal the same temperature dependences of the ESR parameters as those observed for the ferromagnetic crystals. The g -factor shifts remarkably below 15 K, which indicates that the depolymerized crystal undergoes the ferromagnetic phase transition.

IV. DISCUSSION

In the intermediate pressure range, below $P_C = 7$ kbar, the TDAE-C₆₀ monomer partially polymerizes on cooling. Both the polymerization temperature (T_P) and the relative ratio of the polymeric to the monomeric fractions depend on pressure (Fig. 4). Preliminary analysis[19] has suggested that the polymer would have a linear [2+2] cycloadduct bonding structure with a similar intra-chain ball distance as in the case of Rb₁C₆₀ (Ref. [22]). The most prominent difference between the systems is a much larger inter-chain distance in the case of TDAE-C₆₀, which is due to the large size and anisotropic (steric) properties of the TDAE interstitials.

Rich phase diagrams have already been reported for several C₆₀-related compounds. In particular, interesting phase transitions were found for Rb₁C₆₀. Depending on cooling rate and quenching, it can form either monomeric, dimeric[23] or polymeric phases[22][24]. Nevertheless, the coexistence of the two phases has never been observed for Rb₁C₆₀. In contrast, the coexistence of two phases at low temperatures was observed in the case of single-bonded linear polymers of Na₂RbC₆₀ system[25]. In that case, the partial polymerization can be explained by steric effects and by disorder resulting from different possible directions of the bond formation. In contrast, TDAE-C₆₀ is a strongly anisotropic structure with the only one possible direction of the bond forma-

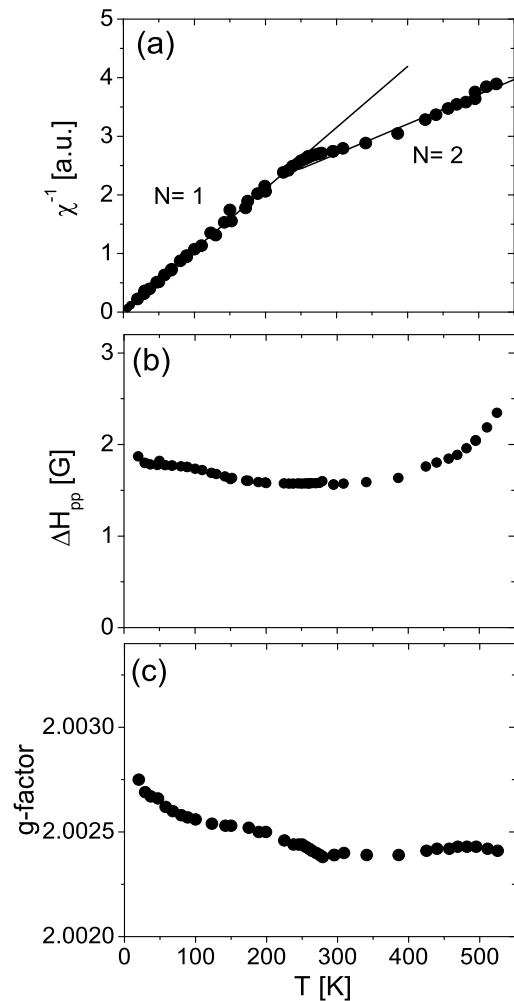


FIG. 6: Temperature dependence of ESR parameters for polymeric β -TDAE- C_{60} phase at ambient pressures: (a) inverse susceptibility (b) linewidth; (c) g -factor. In susceptibility, the onset from simple Curie law is seen above 250 K, but the full appearance of previously silent TDAE⁺ spins is seen at 320 K, leading to doubling of number of spins and appearance of the Weiss constant. The effect is probably connected to structural dynamics of the TDAE dopant.

tion (c-axis). Hence, the partial polymerization is probably governed by the orientation disorder of JTD- C_{60} molecules. The polymerization temperature, T_P , is much lower than the freezing temperature of the C_{60} molecule rotation for a given pressure. This suggests that the freezing of molecular orientations is not sufficient for initiating the polymerization process and there exists a kinetic barrier for this phase transition. It seems to be natural that different kinetic barriers can characterize various relative orientations of the JTD- C_{60} molecules. As the remaining monomeric phase still shows a pronounced ferromagnetic order, most probably, the FM molecular configuration has the highest energetic barrier.

It follows from our measurements that the depoly-

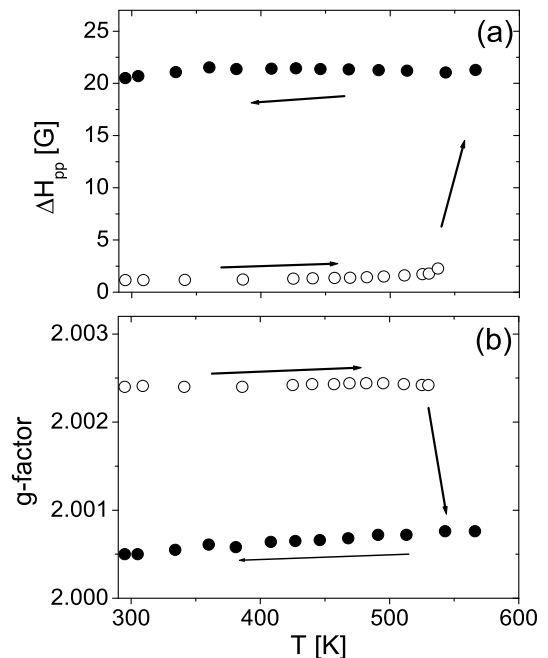


FIG. 7: Temperature dependence of the linewidth and the g -factor of the polymerized crystal in the high-temperature region. The polymeric phase is marked with open circles and the monomeric with closed circles. The full depolymerization is observed above 520 K. At the transition temperature, signals of the both phases are detected, suggesting coexistence of the phases similarly as in the case of partial polymerization.

merization of TDAE- C_{60} occurs at the higher temperature than in the case of one-dimensional A_1C_{60} polymers ($A = K, Rb, Cs$), where, depending on the compound, T_{DP} varies in the range of 300 – 400 K (Ref. [4]). It seems that T_{DP} of TDAE- C_{60} is rather comparable to that found for the two-dimensional polymer Na_4C_{60} ($T_{DP} \approx 500$ K)[26]. Therefore, the polymeric chains of TDAE- C_{60} seem to form much more stable structures than the double-bonded polymeric chains of the Rb_1C_{60} system. If the intra-chain bonds of both TDAE- C_{60} and Rb_1C_{60} were of the same nature (isostructural), one would expect for them similar temperature stability. The observed discrepancy in the temperature stability can be ascribed to a potential structural difference in the two polymeric structures. Alternatively, the previously not investigated effects of dopant molecule and the inter-chain coupling can be important for the polymeric chain stability. A precise structural analysis is needed to answer these questions.

Below room temperature ($T < 260$ K), the ESR spin susceptibility of the polymerized β -phase follows a simple Curie law with one spin $S = 1/2$ per chemical formula. This indicates that spins probed by the ESR experiment are localized. Moreover, in this temperature range, the ESR linewidth for the polymerized β -phase is very narrow (0.5 G) and almost temperature independent, which suggests strong exchange interactions be-

tween the spins. The theoretical band calculations, however, predict that in the absence of electron correlations, the isolated single-charged, double-bonded linear polymer should be metallic with a half-filled band[27]. Also, the same property holds well for single-bonded linear polymers encountered in $\text{Na}_2\text{AC}_{60}$ systems[28]. Indeed, all the other charged linear polymers of the C_{60} compounds, discovered to date, are metallic in a wide temperature range, with possible ground-state instabilities, such as spin-density wave[29]. Therefore, the TDAE- C_{60} polymeric phase seems to be unique.

The inter-chain coupling is very important in alkali fullerenes A_1C_{60} , influencing their dimensionality. However, according to Erwin et al. [27], a direct inter-chain coupling interaction can be neglected in TDAE- C_{60} based on the large inter-chain separation found in these systems.

Assuming a simple model, one would expect the TDAE- C_{60} polymer should be a strongly anisotropic metal. The effective strong localization observed in the β -phase of TDAE- C_{60} might suggest that its actual polymer topology essentially differs from that of Rb_1C_{60} . Alternatively, the localization effect might originate from the possible enhancement of the effective Coulomb repulsion at C_{60} sites, due to the influence of the TDAE⁺ radicals. In such a Mott-Hubbard localization scheme, one would expect a non-vanishing Weiss constant. In contrast, the presence of the Weiss constant has not been detected in the low-temperature β -phase. Mizoguchi et al.[19] suggested that the absence of the Weiss parameter could be explained by re-activation of the positive exchange coupling with the spins of TDAE⁺ radicals. This, in turn, would fortuitously cancel the negative inter- C_{60} spin coupling leading to a diminishing Weiss constant. Nevertheless, in this work, we did not observe the complete recovery of the TDAE⁺ spins in the polymeric phase at the room temperature, as claimed by Mizoguchi et al. Indeed, the appearance of TDAE-spins at elevated temperatures is accompanied with development of the antiferromagnetic Weiss constant.

Assuming that polymeric chains in the β -TDAE- C_{60} have rather small sizes and are disordered, one can apply a model of the random-exchange AFM Heisenberg 1D chains. In this case, the Weiss temperature would be absent, whereas the ESR susceptibility should be proportional to $T^{-\alpha}$, where $\alpha \approx 0.7 - 0.8$. Fitting this model to our data yields $\alpha = 0.96 \pm 0.1$. Clearly, this result does not support the above-mentioned model. For right now, a plausible reason for non-appearance of the Weiss temperature in the polymer phase remains unclear.

As can be seen in Fig. 6a, in the polymeric β -phase,

a complete recovery of the TDAE⁺-related spins is not observed at ambient temperature. The recovery of the spins occurs rather at higher temperatures, with full development at 320 K. The dynamics of the TDAE⁺-related spins is probably connected to small movements of the TDAE⁺ molecules leading to the dimerization shift[13].

V. CONCLUSION

In conclusion, we have investigated the polymerization mechanism in TDAE- C_{60} ferromagnetic system and the physical properties of the polymeric β -phase. The complete polymerization at room temperature is observed at the pressure of 7 kbar. At the same pressure, the ferromagnetic transition is suppressed. Partial polymerization is observed at lower pressures and temperatures, and the stability of the polymeric phase was established in the $P - T$ parameter space. The high depolymerization temperature suggests that the polymeric chains are much more stable than in the case of double-bonded linear polymers of the Rb_1C_{60} systems. To deduce the exact structural properties of the polymer, an additional high-resolution X-ray diffraction study is needed.

Moreover, the observed strong localization of spins in the polymeric TDAE- C_{60} is in contradiction with conclusions from a simple theoretical reasoning and it is not comparable to any other charged linear polymer of the C_{60} . Above 320 K, the previously silent spins on the TDAE- C_{60} are revealed. The observed decoupling of the TDAE⁺ spins is accompanied by the appearance of the Weiss constant.

In summary, we conclude that the polymerization phenomenon in TDAE- C_{60} is very important to better understanding the ferromagnetic properties of the system. However, it can also shed new light towards our general understanding of the ground state electronic properties of the linear fullerenes polymers.

Acknowledgments

This work has been supported in part by a Grant-in-Aid for Scientific research on the priority area "Fullerenes and Nanotubes", from the Japanese Ministry of Education and Culture (T.K., M.F., and K.O.) and by the Polish KBN Grant #2-PO3B-090-19 (A. S.). The support of the Swiss National Scientific Foundation is also greatly acknowledged (S. G. and L. F.).

[1] G. B. Allemand, K. C. Khrmani, A. Koch, F. Wudl, K. Holczer, S. Donovan, G. Gruner, and J. D. Thompson, *Science* **253**, 301 (1991).
 [2] D. Arcon, P. Cevc, A. Omerzu, and R. Blinc, *Phys. Rev. Lett.* **80**, 1529 (1998).

[3] R. Blinc, P. Cevc, D. Arcon, A. Omerzu, M. Mehring, S. Knorr, A. Grupp, A.-L. Barra, and G. Chouteau, *Phys. Rev. B* **58**, 14416 (1998).
 [4] L. Forró and L. Mihály, *Rep. Prog. Phys.* **64**, 649 (2001).
 [5] F. Bommeli, L. Degiorgi, P. Wachter, D. Mihailovic, A.

- Hassanien, P. Venturini, M. Schreiber, and F. Diederich, *Phys. Rev. B* **51**, 1366 (1995).
- [6] A. Schilder, H. Klos, I. Rystau, W. Schütz, and B. Gotschy, *Phys. Rev. Lett.* **73**, 1299 (1994).
- [7] D. P. Arovas and A. Auerbach, *Phys. Rev. B* **52**, 10114 (1995).
- [8] T. Kawamoto, *Solid State Commun.* **101**, 231 (1997).
- [9] G. Sparr, J. D. Thompson, P.-M. Allemand, Q. Li, F. Wudl, K. Holczer, and P.W. Stephens, *Solid State Commun.* **82**, 779 (1992).
- [10] K. Tanaka, A. A. Zakhidov, K. Yoshizawa, K. Okahara, T. Yamabe, K. Yakushi, K. Kikuchi, S. Suzuki, I. Kemoto, and Y. Achiba, *Phys. Lett. A* **164**, 221 (1992).
- [11] K. Tanaka, A. A. Zakhidov, K. Yoshizawa, K. Okahara, T. Yamabe, K. Yakushi, K. Kikuchi, S. Suzuki, I. Kemoto, and Y. Achiba, *Phys. Rev. B* **47**, 7554 (1993).
- [12] T. Kambe, Y. Nogami, and K. Oshima, *Phys. Rev. B* **61**, R862 (2000).
- [13] R. Blinc, K. Pokhodnia, P. Cevc, D. Arcon, A. Omerzu, D. Mihailovic, P. Venturini, L. Golic, Z. Trontelj, J. Luznik, Z. Jeglicic, and J. Pirnat, *Phys. Rev. Lett.* **76**, 523 (1996).
- [14] A. Mrzel, P. Cevc, A. Omerzu, and D. Mihailovic, *Phys. Rev. B* **53**, R2922 (1996).
- [15] B. Narymbetov, A. Omerzu, V. V. Kabanov, M. Tokumoto, H. Kobayashi, and D. Mihailovic, *Nature* **407**, 883 (2000).
- [16] D. Arcon, R. Blinc, P. Cevc, and A. Omerzu, *Phys. Rev. B* **59**, 5247 (1999).
- [17] R. Blinc, P. Jeglič, T. Apih, J. Seliger, D. Arčon, and A. Omerzu, *Phys. Rev. Lett.* **88**, (2002).
- [18] A. Omerzu, M. Tokumoto, B. Tadić, D. Mihailović, *Phys. Rev. Lett.* **87**, 177205 (2001).
- [19] K. Mizoguchi, M. Machino, H. Sakamoto, T. Kawamoto, M. Tokumoto, A. Omerzu, and D. Mihailovic, *Phys. Rev. B* **63**, 140417 (2001).
- [20] A. Sienkiewicz, S. Garaj, R. Gaal, M. Longchamp M. Jaworski C. P. Scholes, and L. Forró, submitted.
- [21] J.-L. Stanger, J.-J. André, P. Turek, Y. Hosokoshi, M. Tamura, M. Kinoshita, P. Rey, J. Cirujeda, and J. Veciana, *Phys. Rev. B* **55**, 8398 (1997).
- [22] P. W. Stephens, G. Bortel, G. Faigel, M. Tegze, A. Janossy, S. Pekker, G. Oszlányi, and L. Forro, *Nature* **370**, 636 (1994).
- [23] G. Oszlányi, G. Bortel, G. Faigel, L. Gránásy, G. M. Bendele, P. W. Stephens, and L. Forró, *Phys. Rev. B* **54**, 11849 (1996).
- [24] S. Pekker, L. Forro, L. Mihaly, and A. Janossy, *Solid State Commun.* **90**, 349 (1994).
- [25] G. M. Bendele, P. W. Stephens, K. Prassides, K. Vavekis, K. Kordatos, and K. Tanigaki, *Phys Rev. Lett.* **80**, 736 (1998).
- [26] G. Oszlányi, G. Baumgartner, G. Faigel, L. Gránásy, and L. Forró, *Phys. Rev. B* **58**, 5 (1998).
- [27] S. C. Erwin, G. V. Krishna, and E. J. Mele, *Phys. Rev. B* **51**, 7345 (1995).
- [28] P. R. Surján, A. Lázár, and M. Kállay, *Phys. Rev. B* **58**, 3490 (1998).
- [29] O. Chauvet, G. Oszlányi, L. Forro, P. W. Stephens, M. Tegze, G. Faigel, and A. Janossy, *Phys. Rev. Lett.* **72**, 2721 (1994).